

## Supporting Information

### **Point-to-Volume Engineering Enables Enhanced Birefringence and Wide Bandgap in Hybrid Halide Ultraviolet Nonlinear Optical Crystals**

Jiajing Wu,<sup>\*a</sup> Ruo-Nan Li,<sup>a</sup> Wen-Dong Yao,<sup>a</sup> Yi-Fan Fu,<sup>a</sup> Sheng-Ping Guo<sup>\*a,b</sup>

<sup>a</sup> Jiangsu Provincial Key Laboratory of Green & Functional Materials and Environmental Chemistry, School of Chemistry and Materials, Yangzhou University, Yangzhou, Jiangsu 225002, P. R. China.

<sup>b</sup> Yunnan Key Laboratory of Electromagnetic Materials and Devices, School of Materials and Energy, Yunnan University, Kunming 650500, P. R. China.

E-mail: [jiajingw@yzu.edu.cn](mailto:jiajingw@yzu.edu.cn), [spguo@yzu.edu.cn](mailto:spguo@yzu.edu.cn)

## Table of Contents

### 1 Experimental Procedures

#### 1.1 Materials

#### 1.2 Synthesis

#### 1.3 Characterizations and Measurements

#### 1.4 Theoretical Calculations

### 2 Results and Discussion

**Table S1.** Crystal data and structural refinement for **MFC** and **MFZC**.

**Table S2.** Fractional atomic coordinates ( $\times 10^4$ ) and equivalent isotropic displacement parameters ( $\text{\AA}^2 \times 10^3$ ) for **MFC** and **MFZC**.  $U_{\text{eq}}$  is defined as 1/3 of the trace of the orthogonalised  $U_{ij}$  tensor.

**Table S3.** Bond lengths for **MFC** and **MFZC**.

**Table S4.** Bond angles for **MFC** and **MFZC**.

**Table S5.** Hydrogen bond lengths ( $\text{\AA}$ ) for **MFC** and **MFZC**.

**Table S6.** Comparison of bandgap, SHG efficiency and birefringence of **MFZC** and the known ionic organic–inorganic hybrid zinc–based halides NLO crystals.

**Figure S1.** Experimental and simulated powder X–ray diffraction patterns of **MFC** and **MFZC**.

**Figure S2.** The asymmetric unit of **MFC**.

**Figure S3.** The crystal structure of **MFC** in the *bc* plane (a) and *ab* plane (d). The *pseudo* layers of **MFZC** viewed along the *c*–axis (b, c).

**Figure S4.** The asymmetric unit of **MFZC**.

**Figure S5.** The crystal structure of **MFZC** in the *bc* plane (a) and *ab* plane (d). The *pseudo* layers of **MFZC** viewed along the *c*–axis (b) and (c).

**Figure S6.** Hydrogen Bond Distribution Ratios of **MFC** (a) and **MFZC** (b).

**Figure S7.** The dihedral angles ( $\gamma$ ) between the organic planes and the principal optical axes plane of **MFC** (a) and **MFZC** (b). The reference plane was calculated based on the entire molecule.

**Figure S8.** The calculated birefringence refractive index of **MFC**.

**Figure S9.** The calculated birefringence refractive index of **MFZC**.

### 3 References

## 1. Experimental Procedures

### 1.1 Materials

zinc oxide (ZnO, 99.9%, Adamas), metformin hydrochloride (C<sub>4</sub>H<sub>12</sub>N<sub>5</sub>Cl, 98%+, Adamas), methanol (MeOH, AR, general reagent), hydrochloric acid (HCl, 40% in water, AR), petroleum ether (AR, general reagent). They were used without further purification.

### 1.2 Syntheses

**Synthesis of MFC SCs.** Firstly, 1 mmol C<sub>4</sub>H<sub>12</sub>N<sub>5</sub>Cl was dissolved in 2 mL HCl at room temperature to form a clarified solution. After the solution had evaporated at room temperature for 20 days, colorless crystals were obtained.

**Synthesis of MFZC SCs.** Firstly, 1 mmol of C<sub>4</sub>H<sub>12</sub>N<sub>5</sub>Cl was dissolved in 5 mL of MeOH to form a colourless solution. Then, ZnO (1 mmol) was dissolved in 1 mL HCl to form a colourless solution. The two precursors were mixed in a 10 mL strain bottle. The resulting solution was allowed to evaporate slowly at room temperature over a period of 15 days to precipitate single crystals.

### 1.3 Characterization and Measurements

Single-crystal X-ray diffraction (SXRD) data were collected on a Bruker D8 QUEST X-ray diffractometer with graphite-monochromated Mo-K $\alpha$  radiation ( $\lambda = 0.71073 \text{ \AA}$ ) at 296.15 K. The crystal structures were solved by dual-space method [1,2] and refined by full-matrix least-squares techniques on F<sup>2</sup> with anisotropic thermal parameters for all atoms. The crystallographic data, atomic coordinates, and equivalent isotropic displacement parameters, bond lengths, bond angles and hydrogen bonds are listed in Tables S1–S5, respectively. The CIF documents were also deposited with the CCDC numbers 2521794 and 2522224.

The powder X-ray diffraction (PXRD) patterns were recorded by using a Bruker D8 Advance diffractometer with Cu-K $\alpha$  radiation ( $\lambda = 1.5406 \text{ \AA}$ ) operating at 40 kV and 100 mA. The simulated patterns were obtained by the Mercury program and single-crystal reflection data.

The UV–Vis–NIR diffuse reflection data were recorded at room temperature using a powdered BaSO<sub>4</sub> sample as a standard (100% reflectance) on a Cary 5000 UV–vis–NIR absorption spectrometer. The scanning wavelength range is from 200 nm to 800 nm. Absorption (K/S) data were calculated from the following Kubelka–Munk function:  $F(R) = (1-R)^2/(2R) = K/S$ ,<sup>[3]</sup> where R is the reflectance, K is the absorption, and S is the scattering.

Second-harmonic generation (SHG) measurements on powder samples of MFC and MFZC were performed using the modified Kurtz–Perry method under a 1064 nm laser, with KDP powder serving as the standard.<sup>[4]</sup> The powder samples were sieved into six different ranges,

including 45–75, 75–110, 110–150, 150–200, 200–250 and 250–315  $\mu\text{m}$  to measure their size-dependent SHG responses. The SHG signals were detected using photomultiplier tube and recorded via a digital oscilloscope.

#### 1.4 Theoretical calculations

The single-crystal structural data of **MFC** and **MFZC** were used for theoretical calculations. The electronic structures and optical properties were calculated using a plane-wave basis set and pseudo-potentials within density functional theory (DFT) were implemented in the total-energy CASTEP code.<sup>[5]</sup> Perdew–Burke–Ernzerh (PBE) in the generalized gradient approximation (GGA) was chosen for the exchange and correlation functions.<sup>[6]</sup> The norm-conserving pseudopotential described the interactions between the ionic cores and the electrons. The following valence–electron configurations were considered in the computation: Zn–3p<sup>6</sup>3d<sup>10</sup>4s<sup>2</sup>, C–2s<sup>2</sup>2p<sup>2</sup>, N–2s<sup>2</sup>2p<sup>3</sup>, and H–1s<sup>1</sup>. A planewave cutoff energy of 830 eV (**MFC**) and 350 eV (**MFZC**), and  $2 \times 2 \times 1$  (**MFC**) and  $4 \times 4 \times 2$  (**MFZC**) grid of Monkhorst–Pack points were employed for bandgap structure and density of states calculation, which ensured good convergence of the computed structures and energies. The other parameters and convergence criteria are default values for the CASTEP code.

The polarizability anisotropy of **MFC** and **MFZC** were calculated using the Gaussian 09 with PBE0–def2–QZVPD basis sets at the molecular level.<sup>[7,8]</sup> Wavefunction analyses were conducted utilizing the Multiwfn program.<sup>[9,10]</sup>

## 2. Results and Discussion

Table S1. Crystal data and structural refinement for MFC and MFZC.

Compound	MFC	MFZC
<b>Empirical formula</b>	$C_4H_{13}N_5Cl_2$	$(C_4H_{13}N_5)ZnCl_4$
<b>Formula weight/g mol<sup>-1</sup></b>	202.09	338.36
<b>Temperature/K</b>	296.15	296.15
<b>Crystal system</b>	monoclinic	monoclinic
<b>Space group</b>	$P2_1$	$P2_1$
<i>a</i> /Å	7.1245(5)	6.8052(6)
<i>b</i> /Å	5.7932(4)	6.9176(5)
<i>c</i> /Å	12.5446(8)	14.1930(12)
$\alpha$ /°	90	90
$\beta$ /°	105.077(2)	98.816(3)
$\gamma$ /°	90	90
<b>Volume/Å<sup>3</sup></b>	499.94(6)	660.25(9)
<i>Z</i>	2	2
$\rho_{calc}$ (g/cm <sup>3</sup> )	1.343	1.702
$\mu$ /mm <sup>-1</sup>	0.603	2.643
<b>F(000)</b>	212.0	340.0
<b>2<math>\theta</math> range (deg)</b>	5.922 – 54.93	6.058 – 55.056
<b>Index ranges</b>	$-9 \leq h \leq 9, -7 \leq k \leq 7, -16 \leq l \leq 16$	$-8 \leq h \leq 8, -8 \leq k \leq 8, -18 \leq l \leq 16$
<b>Reflections collected</b>	7342	10700
<b>Independent reflections</b>	2262	3020
	[ $R_{int} = 0.0305, R_{sigma} = 0.0381$ ]	[ $R_{int} = 0.0365, R_{sigma} = 0.0395$ ]
<b>GOF on F<sup>2</sup></b>	1.050	1.030
<b>Final R indexes [<math>I \geq 2\sigma(I)</math>]</b>	$R_1 = 0.0330, wR_2 = 0.0680$	$R_1 = 0.0231, wR_2 = 0.0475$
<b>Final R indexes [all data]</b>	$R_1 = 0.0439, wR_2 = 0.0715$	$R_1 = 0.0268, wR_2 = 0.0484$
$\Delta\rho_{max}, \Delta\rho_{min}$ /e Å <sup>-3</sup>	0.24/−0.18	0.22/−0.36

$R1 = \frac{||F_o| - |F_c||}{|F_o|}$ ;  $wR2 = \frac{[w(F_o^2 - F_c^2)^2]}{[w(F_o^2)^2]^{1/2}}$ .  $w = 1/[\sigma^2(F_o^2)+(0.0352P)^2 + 0.0348P]$   
and  $P = (F_o^2+2F_c^2)/3$  for **MFC**.  $w = 1/[\sigma^2(F_o^2)+(0.0149P)^2]$  and  $P = (F_o^2+2F_c^2)/3$  for **MFZC**.

**Table S2.** Fractional atomic coordinates ( $\times 10^4$ ) and equivalent isotropic displacement parameters ( $\text{\AA}^2 \times 10^3$ ) for **MFC** and **MFZC**.  $U_{\text{eq}}$  is defined as 1/3 of the trace of the orthogonalised  $U_{ij}$  tensor.

Atom	$x$	$y$	$z$	$U_{\text{eq}}$
<b>MFC</b>				
Cl (1)	13333.2(10)	4205.1(13)	5510.7(6)	36.0(2)
Cl (2)	10706.0(11)	10513.4(13)	8571.1(6)	42.4(2)
N (1)	10685(3)	6062(4)	7078(2)	38.3(7)
N (2)	8425(3)	5059(4)	8785.8(19)	36.8(6)
N (3)	7413(3)	5529(5)	6902.2(18)	34.0(6)
N (4)	6108(4)	7808(4)	8044(2)	34.2(6)
N (5)	8931(4)	3648(4)	5756(2)	38.7(7)
C (1)	7348(4)	6191(5)	7949(2)	28.5(6)
C (2)	9056(4)	5066(5)	6584(2)	30.8(7)
C (3)	5294(4)	9475(6)	7167(3)	43.4(8)
C (4)	5834(6)	8384(8)	9122(3)	59.4(12)
<b>MFZC</b>				
Zn (1)	-2775.5(4)	6174.7(5)	2043.2(2)	27.92(10)
Cl (1)	-4819.1(10)	4705.5(12)	856.7(5)	35.11(18)
Cl (2)	191.1(10)	6405.5(12)	1493.7(5)	33.52(17)
Cl (3)	-2266.1(11)	4328.0(12)	3391.9(5)	37.18(19)
Cl (4)	-3915.1(11)	9132.5(12)	2412.1(7)	44.0(2)
N (1)	-1355(3)	1295(5)	666.4(17)	40.0(6)
N (2)	2007(4)	876(5)	880.4(17)	37.5(7)
N (3)	357(3)	1193(4)	2182.7(14)	27.5(5)
N (4)	2143(4)	930(5)	3703.5(17)	37.3(6)
N (5)	3105(4)	3112(4)	2645.8(18)	33.3(6)
C (1)	359(4)	1129(5)	1214.7(18)	27.1(6)
C (2)	1919(4)	1754(4)	2853(2)	25.3(6)
C (3)	3565(6)	1756(7)	4476(2)	70.0(15)
C (4)	1133(7)	-864(7)	3897(3)	82.0(17)

**Table S3.** Bond lengths for **MFC** and **MFZC**.

<b>Atom</b>	<b>Atom</b>	<b>Length/Å</b>	<b>Atom</b>	<b>Atom</b>	<b>Length/Å</b>
<b>MFC</b>					
N (1)	C (2)	1.300(3)	N (4)	C (1)	1.314(4)
N (2)	C (1)	1.304(3)	N (4)	C (3)	1.465(4)
N (3)	C (1)	1.381(3)	N (4)	C (4)	1.455(4)
N (3)	C (2)	1.358(3)	N (5)	C (2)	1.309(4)
<b>MFZC</b>					
Zn (1)	Cl (1)	2.2550(8)	N (3)	C (1)	1.375(3)
Zn (1)	Cl (2)	2.2786(7)	N (3)	C (2)	1.370(3)
Zn (1)	Cl (3)	2.2831(8)	N (4)	C (2)	1.322(4)
Zn (1)	Cl (4)	2.2774(8)	N (4)	C (3)	1.463(4)
N (1)	C (1)	1.304(3)	N (4)	C (4)	1.465(5)
N (2)	C (1)	1.295(4)	N (5)	C (2)	1.301(4)

**Table S4.** Bond angles for **MFC** and **MFZC**.

<b>Atom</b>	<b>Atom</b>	<b>Atom</b>	<b>Angle/°</b>	<b>Atom</b>	<b>Atom</b>	<b>Atom</b>	<b>Angle/°</b>
<b>MFC</b>							
C (2)	N (3)	C (1)	125.4(2)	N (2)	C (1)	N (4)	123.7(3)
C (1)	N (4)	C (3)	123.1(2)	N (4)	C (1)	N (3)	118.3(2)
C (1)	N (4)	C (4)	120.2(3)	N (1)	C (2)	N (3)	120.2(3)
C (4)	N (4)	C (3)	115.1(3)	N (1)	C (2)	N (5)	121.7(3)
N (2)	C (1)	N (3)	117.9(3)	N (5)	C (2)	N (3)	118.1(3)
<b>MFZC</b>							
Cl (1)	Zn (1)	Cl (2)	104.68(3)	C (2)	N (4)	C (4)	123.0(3)
Cl (1)	Zn (1)	Cl (3)	111.77(3)	C (3)	N (4)	C (4)	117.8(3)
Cl (1)	Zn (1)	Cl (4)	112.57(3)	N (1)	C (1)	N (3)	117.1(2)
Cl (2)	Zn (1)	Cl (3)	107.31(3)	N (2)	C (1)	N (1)	122.6(2)
Cl (4)	Zn (1)	Cl (2)	111.50(3)	N (2)	C (1)	N (3)	120.3(2)
Cl (4)	Zn (1)	Cl (3)	108.86(3)	N (4)	C (2)	N (3)	118.7(3)
C (2)	N (3)	C (1)	125.7(2)	N (5)	C (2)	N (3)	119.3(3)
C (2)	N (4)	C (3)	119.0(3)	N (5)	C (2)	N (4)	122.0(3)

**Table S5.** Hydrogen bond lengths (Å) for **MFC** and **MFZC**.

D–H	d(D–H)	d(H...A)	d(D...A)	∠(D–H...A)(°)	A
<b>MFC</b>					
N (1) – H (1A)	0.86	2.47	3.246(3)	150	Cl (2)
N (1) – H (1B)	0.86	2.54	3.228(3)	137	Cl (2)
N (2) – H (2A)	0.86	2.46	3.242(2)	151	Cl (2)
N (2) – H (2B)	0.86	2.37	3.185(2)	159	Cl (1)
N (3) – H (3)	0.86	2.25	3.073(2)	162	Cl (2)
N (4) – H (4B)	0.86	2.41	3.222(2)	159	Cl (1)
N (4) – H (4B)	0.86	2.31	3.143(2)	163	Cl (1)
C (3) – H (3C)	0.96	2.83	3.738(4)	159	Cl (2)
C (4) – H (4D)	0.96	2.79	3.746(4)	172	Cl (1)
<b>MFZC</b>					
N (1) – H (1A)	0.86	2.47	3.282(2)	157	Cl (2)
N (1) – H (1B)	0.86	2.77	3.375(3)	129	Cl (4)
N (2) – H (2A)	0.86	2.75	3.490(3)	146	Cl (2)
N (2) – H (2A)	0.86	2.79	3.441(3)	134	Cl (4)
N (2) – H (2B)	0.86	2.65	3.469(3)	159	Cl (1)
N (3) – H (3)	0.86	2.48	3.299(2)	158	Cl (1)
N (4) – H (4A)	0.86	2.53	3.276(3)	145	Cl (3)
N (4) – H (4B)	0.86	2.72	3.287(3)	125	Cl (2)
N (4) – H (4B)	0.86	2.61	3.280(3)	136	Cl (4)
C (4) – H (4D)	0.96	2.74	3.685(4)	168	Cl (3)

**Table S6.** Comparison of bandgap, SHG efficiency and birefringence of **MFZC** and the known ionic organic–inorganic hybrid zinc–based halides NLO crystals.

<b>Compound</b>	<b>Space Group</b>	<b>Bandgap (eV)</b>	<b>SHG (<math>\times</math>KDP)</b>	<b>Phase matchable</b>	<b>Calculated birefringence</b>	<b>References</b>
(3–QUO) <sub>2</sub> ZnI <sub>4</sub>	<i>Pmn2</i> <sub>1</sub>	3.94	0.6	No	0.050@546nm	[11]
(4–AMP)ZnBr <sub>4</sub> ·H <sub>2</sub> O	<i>P2</i> <sub>1</sub>	3.84	2.1	Yes	0.053@546nm	[12]
(4–AMP)ZnCl <sub>4</sub> ·H <sub>2</sub> O	<i>P2</i> <sub>1</sub>	3.94	1.3	Yes	0.069@546nm	[12]
(C <sub>4</sub> H <sub>11</sub> N <sub>2</sub> )ZnI <sub>3</sub>	<i>Cc</i>	4.52	2.1	Yes	0.080@546nm	[13]
(3–AMP)ZnCl <sub>4</sub>	<i>Cmc2</i> <sub>1</sub>	4.88	2.05	Yes	0.144@546nm	[14]
(3–AMP)ZnBr <sub>4</sub>	<i>Cmc2</i> <sub>1</sub>	4.64	4.36	Yes	0.129@546nm	[14]
(C <sub>13</sub> N <sub>3</sub> H <sub>14</sub> ) <sub>2</sub> ZnBr <sub>4</sub>	<i>Pna2</i> <sub>1</sub>	3.96	1.12	Yes	0.150@1064nm	[15]
(C <sub>6</sub> H <sub>5</sub> N <sub>2</sub> ) <sub>2</sub> ZnCl <sub>4</sub>	<i>P2</i> <sub>1</sub> <i>2</i> <sub>1</sub> <i>2</i> <sub>1</sub>	3.83	1.2	Yes	0.223@546nm	[16]
ZnBr(C <sub>6</sub> H <sub>3.5</sub> FNO <sub>2</sub> ) <sub>2</sub>	<i>P2</i> <sub>1</sub> <i>2</i> <sub>1</sub> <i>2</i>	4.2	1.7	Yes	0.300@532nm	[17]
(C <sub>14</sub> H <sub>14</sub> N <sub>2</sub> )ZnCl <sub>4</sub>	<i>Cm</i>	3.25	1.63	Yes	0.325@1064nm	[18]
<b>MFZC</b>	<i>P2</i> <sub>1</sub>	4.72	2.2	Yes	0.090@546nm	This work

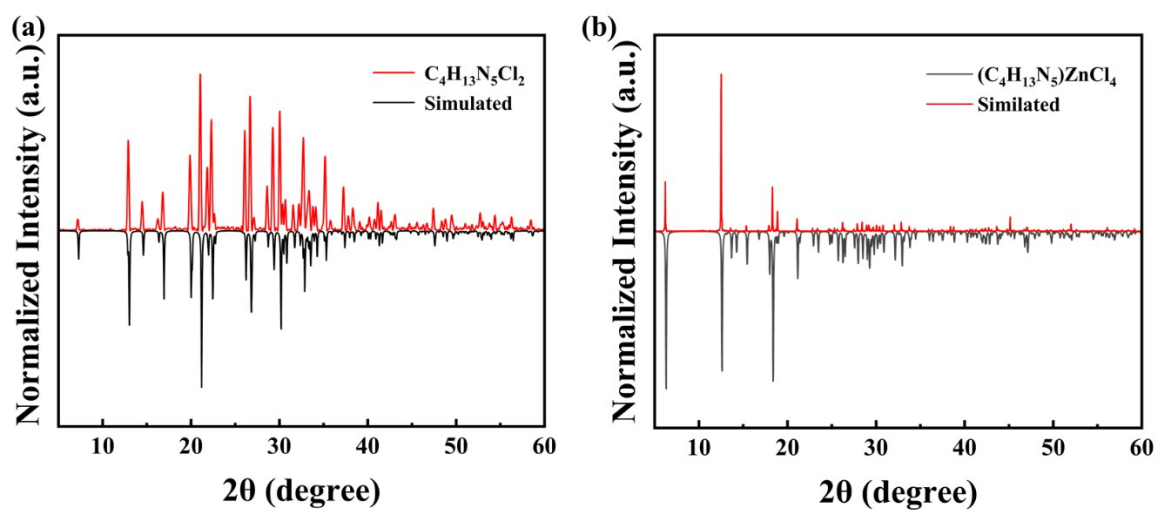


**Figure S1.** Experimental and simulated powder X-ray diffraction patterns of MFC (a) and MFZC (b).

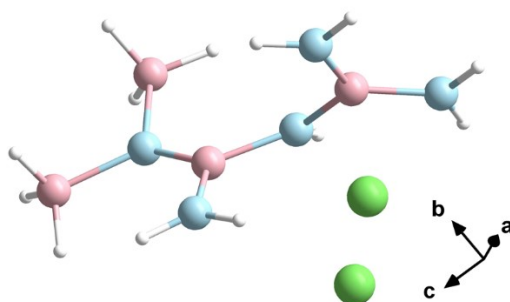


**Figure S2.** The asymmetric unit of MFC.

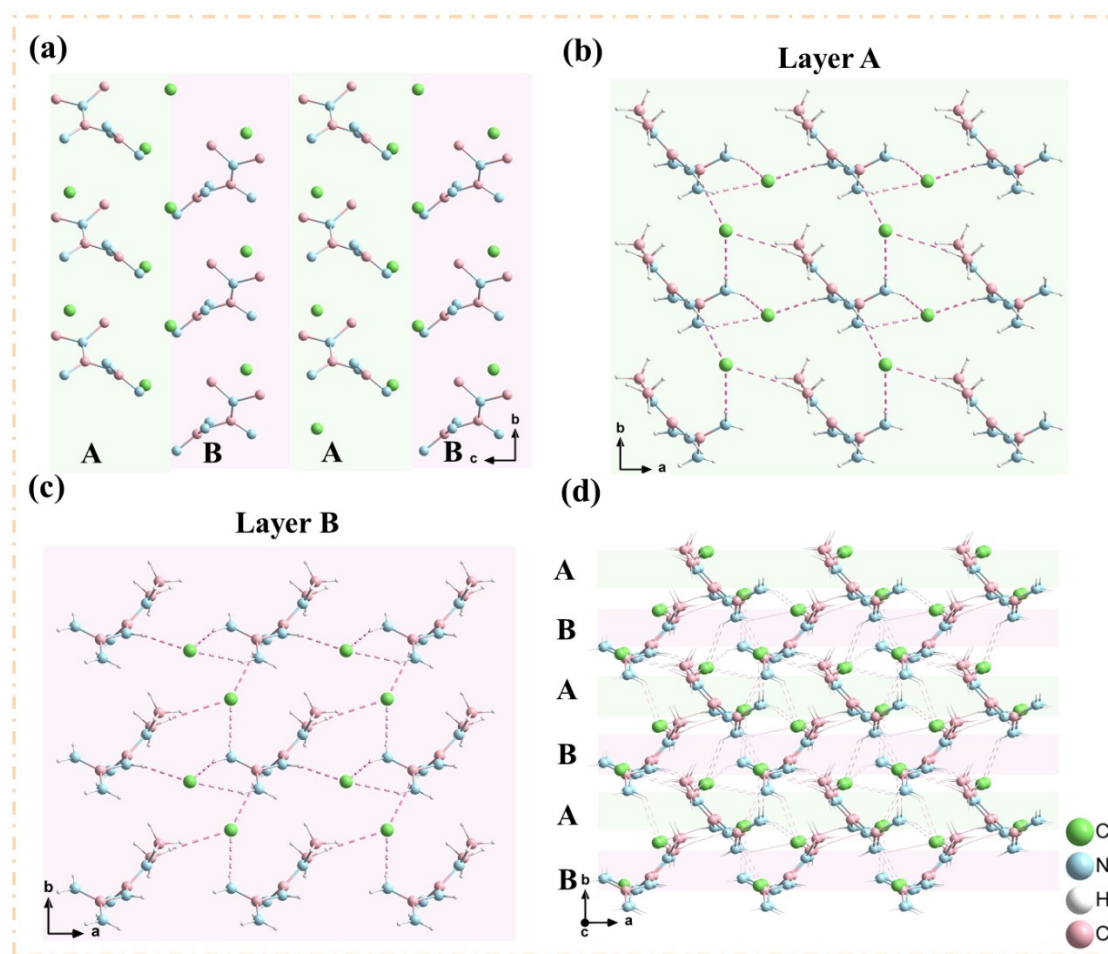


**Figure S3.** The crystal structure of MFC in the  $bc$  plane (a) and  $ab$  plane (d). The *pseudo* layers of MFC viewed along the  $c$ -axis (b, c).

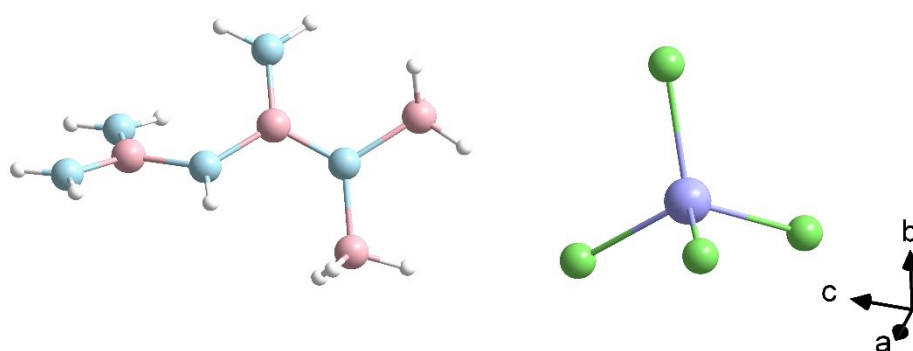


**Figure S4.** The asymmetric unit of MFZC.

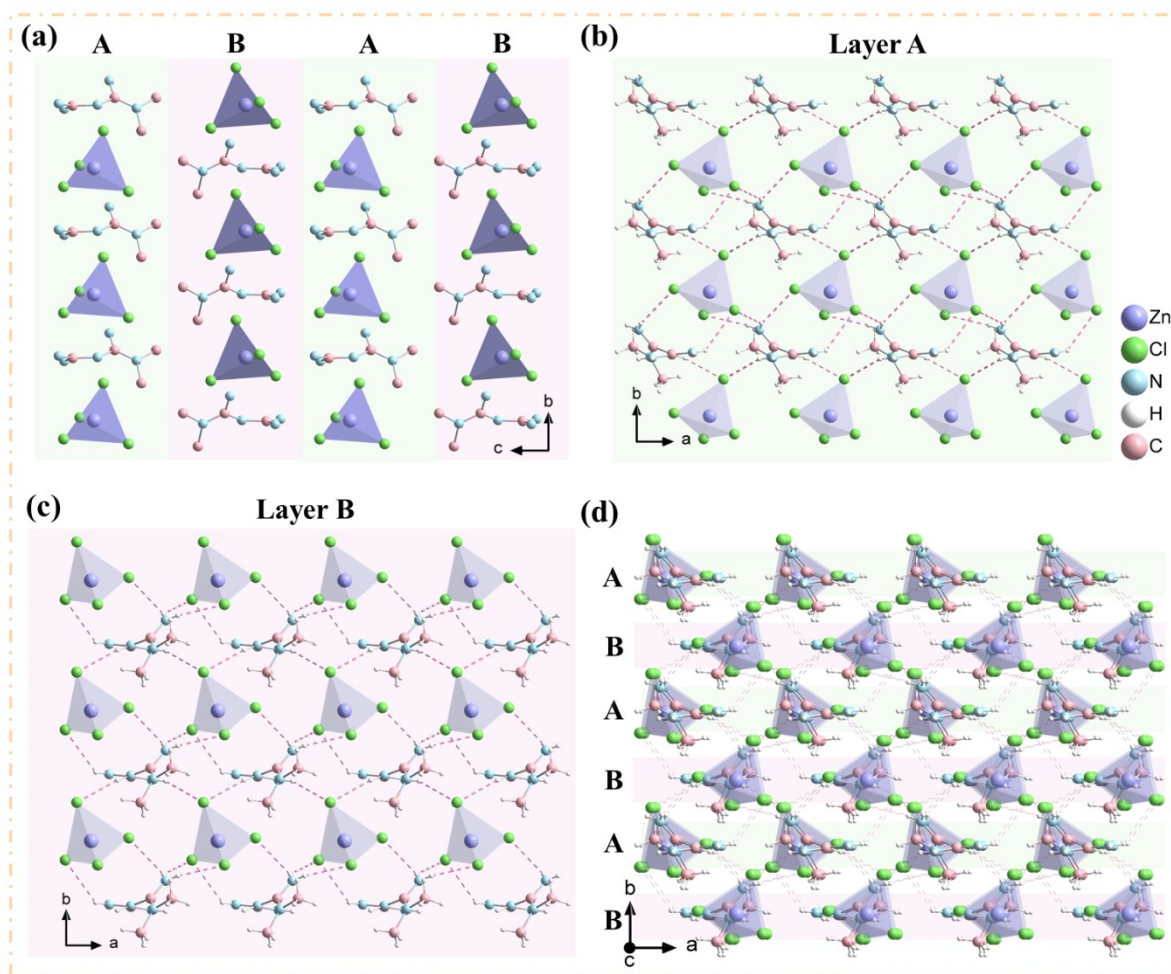


**Figure S5.** The crystal structure of MFZC in the *bc* plane (a) and *ab* plane (d). The *pseudo* layers of MFZC viewed along the *c*-axis (b, c).

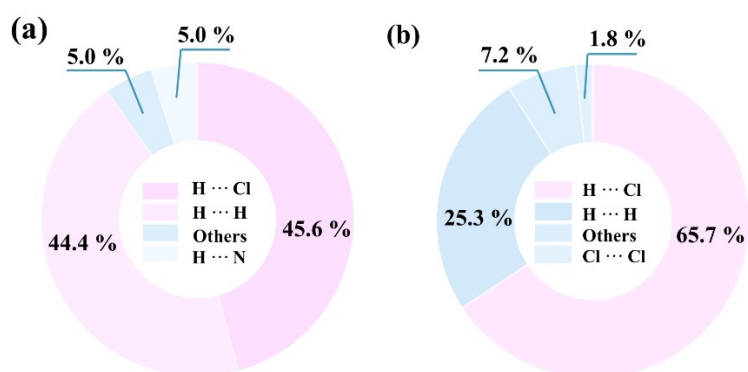


**Figure S6.** Hydrogen Bond Distribution Ratios of MFC (a) and MFZC (b).

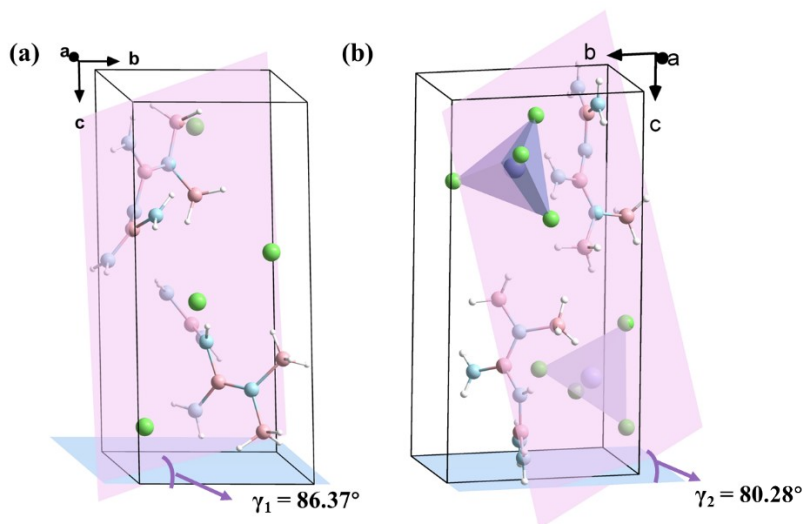


**Figure S7.** The dihedral angles ( $\gamma$ ) between the organic planes and the principal optical axes plane of **MFC** (a) and **MFZC** (b). The reference plane was calculated based on the entire molecule.

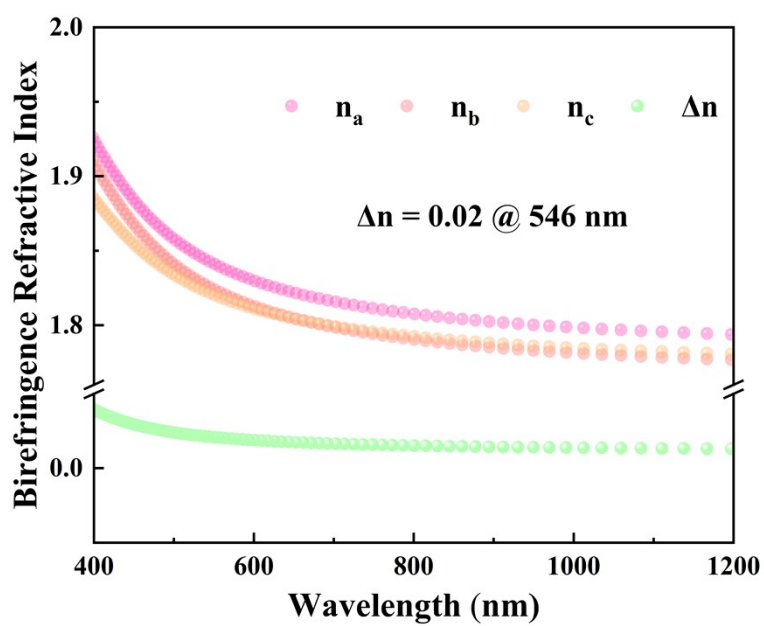


**Figure S8.** The calculated birefringence refractive index of **MFC**.

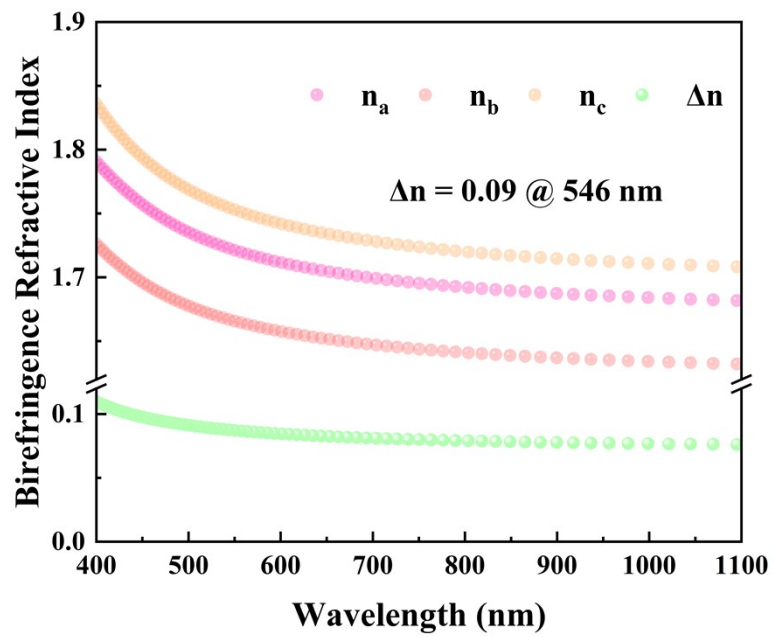


**Figure S9.** The calculated birefringence refractive index of MFZC.

### 3. References

- [1]. O. V. Dolomanov, L. J. Bourhis, R. J. Gildea, J. A. K. Howard, H. Puschman, *J. Appl. Crystallogr.*, 2009, **42**, 339–341.
- [2]. G.M Sheldrick, *Acta Crystallogr. C.*, 2015, **71**, 3–8.
- [3]. J. Tauc, *Mater. Res. Bull.* 1970, **5**, 721–729.
- [4]. S. K. Kurtz and T. T. Perry, *J. Appl. Phys.*, 1968, **39**, 3798–3813.
- [5]. M. D. Segall, P. L. D. Lindan, M. J. Probert, C. J. Pickard, P. J. Hasnip, S. J. Clark and M. C. Payne, Preface, *J. Phys.: Condens. Matter.*, 2002, **14**, 2717–2744.
- [6]. J. P. Perdew, K. Burke, M. Ernzerhof, *Phys. Rev. Lett.*, 1996, **77**, 3865–38685.
- [7]. C. Adamo, V. Barone, *J. Chem. Phys.*, 1999, **110**, 6158–6170.
- [8]. D. Rappoport, F. Furche, *J. Chem. Phys.*, 2010, **133**, 134105.
- [9]. T. Lu, F. Chen, *J. Comput. Chem.*, 2012, **33**, 580–592.
- [10]. T. Lu, *J. Chem. Phys.*, 2024, **161**, 082503.
- [11]. M.–C. Wang, Z. Lin, J.–J. Li, J.–M. Lian, Y.–X. Hu, Y. Chen, K.–Z. Du, J. Chen, *Chin. Chem. Lett.*, 2025, 111639.
- [12]. C. Shen, C. Zhang, Q. Xing, D. Sun, K. Wu, B. Zhang, J. Wang, D. Wang, *Chem. Eng. J.* 2025, **509**, 161389.
- [13]. J. Chen, H.–Y. Wu, M.–B. Xu, M.–C. Wang, Q.–Q. Chen, B.–X. Li, C.–L. Hu, K.–Z. Du, *Inorg. Chem. Front.*, 2024, **11**, 5587–5597.
- [14]. C. Shen, J. Liu, D. Sun, K. Yang, B. Zhang, K. Wu, J. Wang, D. Wang, *Small*, 2025, **21**, 2501471.
- [15]. J. Wu, Y.–F. Fu, W. Liu, and S.–P. Guo, *Inorg. Chem. Front.*, 2024, **11**, 7090–7097.
- [16]. D.–X. Yang, Y.–L. Lv, J.–D. Guo, W.–Y. Gao, W Liu, R.–L Tang, *Inorg. Chem.*, 2025, **64**, 3643–3648.
- [17]. Q. Zhu, Y. Tao, C. Yang, J. Gou, Y. Zhu, X. Wang, Q. Wu, *Inorg. Chem.*, 2024, **63**, 22620–22627.
- [18]. X. Li, P. Gong, M. Chen, S. Zhuang, M. Qi, W. Wang, X. Wang, Zhen Jia, and M. Xia, *Inorg. Chem. Front.*, 2025, **12**, 7675–7683.